J. Fluid Mech. (1994), *vol.* 263, *pp.* 133–150

On the stability of Poiseuille flow of a Bingham fluid

By I. A. FRIGAARD,[1] S. D. HOWISON[2] AND I. J. SOBEY[3]

[1] Industriemathematik, Institut für Mathematik, Johannes Kepler Universität, A-4040, Linz, Austria

[2] Mathematical Institute, University of Oxford, 24–29, St. Giles, Oxford, OX1 3LB, UK

[3] Oxford University Computing Laboratory, 8–11, Keble Road, Oxford, OX1 3QD, UK

(Received 9 June 1992 and in revised form 25 August 1993)

The stability to linearized two-dimensional disturbances of plane Poiseuille flow of a Bingham fluid is considered. Bingham fluids exhibit a yield stress in addition to a plastic viscosity and this description is typically applied to drilling muds. A non-zero yield stress results in an additional parameter, a Bingham number, and it is found that the minimum Reynolds number for linear instability increases almost linearly with increasing Bingham number.

1. Introduction

Drilling muds are used in the oil industry to provide lubrication and cooling to the drill bit, to carry rock cuttings to the surface and to provide hydrostatic containment of formation fluids. The muds are a mixture of water (possibly emulsified with oil), weighting material and clay, as well as small quantities of salts and polymeric fluid loss additives. This physical makeup leads to complex rheological behaviour with the muds showing strong non-Newtonian stress/strain-rate relationships. As only small quantities of polymer are present, the major feature of the stress/strain-rate relationship is that of an inelastic non-Newtonian fluid.

The source of inelastic non-Newtonian behaviour lies in both the fluid/solid mixture and in the ability of clay particles to cross-link chemically, forming bonds between particles. This produces a range of non-Newtonian behaviour depending on the extent and rate of cross-link formation. Once links have formed the mud resists motion until a yield stress is reached, at which point the cross-links are mechanically broken and the mud behaves as a fluid. In the period before the yield stress is reached it is not known whether the mud undergoes creep or elastic deformation but one would expect a variety of possibilities, depending on the type of mud and the timescale over which the stress is built up. Once the yield stress is exceeded the mud viscosity may vary considerably with changing strain rate. If the fluid is brought back below the yield stress, cross-links again dominate and the fluid gels and becomes solid. The process of cross-link formation and destruction is not instantaneous and drilling muds show extensive thixotropic properties. In this paper thixotropy will not be considered and the internal cross-linking process is idealized as happening instantaneously. In the simplest model of this type of fluid, the excess deviatoric stress over the yield stress is assumed to be a linear function of the shear rate. Such fluids are called Bingham fluids and this description is used widely in oilfield calculations.

Oldroyd (1947) formulated the constitutive relations between stress, strain and strain rate by assuming an elastic response below the yield stress and an inelastic response

above the yield stress. In a viscometric-type flow with displacement $\hat{v}(\hat{y}, \hat{t})$ and velocity $\hat{u}(\hat{y}, \hat{t})$ in the $\hat{x}$-direction, the deviatoric stress $\hat{\tau}$ is given by

$$\hat{\tau} = E\partial\hat{v}/\partial\hat{y}$$

when $\hat{\tau} < \tau_0$, where τ_0 is the yield stress, and by

$$\hat{\tau} = \tau_0 + \mu_0 \partial\hat{u}/\partial\hat{y}$$

when $\hat{\tau} > \tau_0$. E is the Young's modulus and μ_0 is the (limiting) fluid viscosity. More recently the elastic behaviour has been neglected and it is assumed that the strain rate vanishes when the stress is below the yield stress, (e.g. Beris *et al.* 1985; Walton & Bittleston 1991). In this paper the latter formulation is followed.

Since drilling muds are used to carry cuttings from the drill face to the surface it is important to know the nature of the fluid motion in the annulus between the drill collars or drill pipe and the well bore. In particular it is essential to know whether the flow is laminar or turbulent. Under certain circumstances the annulus can be approximated as a two-dimensional channel. The stability of such channel flows is then an important design feature in any pumping strategy.

For Newtonian fluids the stability of plane Poiseuille flow has received considerable attention. Two-dimensional, linear perturbations result in the instability of plane Poiseuille flow for Reynolds numbers, R, such that $R > R_c \approx 5772$; see e.g. Orszag (1971). The Reynolds number here is based on the maximum fluid velocity and the channel half-width. Weakly nonlinear stability theories (and extensions) have indicated that instability can result from sufficiently large-amplitude finite perturbations for Reynolds numbers above ≈ 2900; e.g. Zahn *et al.* (1974); Herbert (1976). In contrast, laboratory results have shown instability to finite-amplitude disturbances for Reynolds numbers as low as 1000, e.g. Davies & White (1928); Patel & Head (1969).

The apparent discrepancy between theoretical and experimental values has more recently been explained by Orszag and co-workers; see Orszag & Kells (1980), Orszag & Patera (1983). Orszag & Patera considered the three-dimensional linear stability of a finite, two-dimensional perturbation to the laminar flow. For Reynolds numbers greater than about 2900 the nonlinear instability of the laminar solution allows such two-dimensional perturbations to be sustained. For $R < 2900$, although finite perturbations are predicted to decay, the decay occurs on a relatively slow timescale, ($\sim R$), and this allows time for rapid growth of the three-dimensional linear perturbations to occur. This analysis has been able to predict critical Reynolds numbers of about 1000, for moderate amplitudes of the two-dimensional disturbances. More importantly, the growth rates predicted for the secondary three-dimensional instability are much larger than those that are predicted for linear two-dimensional Orr–Sommerfeld modes, and are characteristic of the convective timescale of the basic flow. This fits well with the rapid subcritical transition to turbulence, which is observed to take place over a few channel widths, in plane Poiseuille flow.

The stability of plane Poiseuille flow of a Bingham fluid has received very little attention to date. In Bingham fluids the non-dimensional ratio of the yield stress and the viscous stress is referred to as the Bingham number. Experimental work by Pratt, reported in Hanks & Pratt (1967), shows a massive increase in transitional Reynolds number from about 1400 to about 26700, as the Bingham number is increased from about 0.45 to about 560. These Reynolds and Bingham numbers are based upon the maximum fluid velocity, the limiting viscosity, μ_0, and the channel half-width. Similarly significant increases in transitional Reynolds number with Bingham number are observed in pipe flows, for which there is much more experimental data, e.g. Thomas

(1960). However, the viscosity of a Bingham fluid varies with the rate of strain. Use of an effective viscosity scale, the mean fluid velocity and an effective pipe diameter as a lengthscale results in transitional Reynolds numbers which lie in the range 2000–3000 for pipe, annulus and channel geometries. Hanks and co-workers have formulated an empirically based theory to predict transitional Reynolds numbers and friction factor/Reynolds number curves for the flow of Bingham fluids in these geometries, e.g. Hanks (1963), Hanks & Pratt (1967), Hanks & Dadia (1971). It is essentially this theory that is used for many oil flow calculations (e.g. Dowell Schlumberger 1985).

Although extremely useful for engineering purposes, such theories do not begin to address the mathematical issues. When departures are made from the Newtonian model of a fluid it is particularly important that issues such as stability are addressed from a mathematical/theoretical viewpoint, as well as from an empirical one. The Bingham model is highly idealized, and usually approximates a more complex fluid rheology. Thus, the proper interpretation of empirical results always depends on the effectiveness of this approximation.

This paper considers the stability to small disturbances of Poiseuille flow of a Bingham fluid in a two-dimensional channel. This is the first step that should be taken in developing a more complete mathematical understanding of the instability of such flows. Although transition for a Poiseuille flow of a Bingham fluid is likely to be subcritical, there is no guarantee. The linearized theory developed here will underlie weakly nonlinear theories such as have been developed for Newtonian fluids. Additionally, the linear critical Reynolds number is of interest, since it forms an upper bound (on R) for the flow's stability, and gives insight into how fluid stability is affected by a yield stress.

An outline of the remainder of the paper is as follows. In §2 the equations of motion for a Bingham fluid are formulated and the basic unperturbed Poiseuille flow is described. In §3 the linear stability of the basic flow is considered, and the numerical solution of the stability problem is given in §4. In §5 the results and their applicability are briefly discussed.

2. The Bingham model of Poiseuille flow

As indicated above, the tensorial forms of the constitutive equations that will be used for a Bingham fluid are

$$\begin{aligned} \hat{\boldsymbol{\tau}} &= \hat{\eta}\hat{\dot{\boldsymbol{\gamma}}} \Leftrightarrow \hat{\tau} \geqslant \tau_0, \\ \hat{\dot{\gamma}} &= 0 \Leftrightarrow \hat{\tau} < \tau_0, \end{aligned} \tag{1}$$

where a hat denotes a dimensional variable, and where $\hat{\dot{\boldsymbol{\gamma}}}$ and $\hat{\boldsymbol{\tau}}$ are the rate-of-strain and deviatoric stress tensors respectively. The yield stress is denoted by τ_0 and $\hat{\eta}$ denotes the effective viscosity, defined by

$$\hat{\eta} = \mu_0 + \tau_0 \hat{\dot{\gamma}}^{-1}; \tag{2}$$

$\hat{\dot{\gamma}}$ and $\hat{\tau}$ are respectively the second invariants of the rate-of-strain and deviatoric stress tensors. They are given by

$$\hat{\dot{\gamma}} = [\tfrac{1}{2}\hat{\dot{\gamma}}_{ij}\hat{\dot{\gamma}}_{ij}]^{\frac{1}{2}}, \tag{3}$$

$$\hat{\tau} = [\tfrac{1}{2}\hat{\tau}_{ij}\hat{\tau}_{ij}]^{\frac{1}{2}}. \tag{4}$$

Denoting by $\hat{p}$, ρ, $\hat{\boldsymbol{u}}$ and $\hat{\boldsymbol{\sigma}}$ the fluid pressure, density, velocity vector and stress tensor respectively, the full equations of motion for a Bingham fluid in the absence of external forces are

$$\hat{\boldsymbol{\nabla}} \cdot \hat{\boldsymbol{u}} = 0, \tag{5}$$

$$\rho[\hat{\boldsymbol{u}}_{\hat{t}} + (\hat{\boldsymbol{u}} \cdot \hat{\boldsymbol{\nabla}})\hat{\boldsymbol{u}}] = \hat{\boldsymbol{\nabla}} \cdot \hat{\boldsymbol{\sigma}}(\hat{p}, \hat{\boldsymbol{u}}), \tag{6}$$

$$\hat{\boldsymbol{\sigma}} = -\hat{p}\boldsymbol{\delta} + \hat{\boldsymbol{\tau}}, \tag{7}$$

where δ is the Kronecker delta. At the boundaries of the flow region the usual 'no-slip' conditions will hold.

These equations are satisfied everywhere in the fluid. However, in regions where the yield stress is not exceeded the stress tensor will be indeterminate. In these regions, the rate-of-strain tensor is identically zero. Hence, such regions behave as would a rigid solid. These regions are called 'plug' regions. Boundaries of plug regions are located via the yield criterion

$$\hat{\tau} = \tau_0. \tag{8}$$

The motion of a plug region, Ω_s, is determined by conservation of momentum. Conservation of linear momentum is represented by

$$\oint_{\partial\Omega_s} \hat{\sigma}_{i,j} n_j \, \mathrm{d}s = \int_{\Omega_s} \rho \frac{\mathrm{d}}{\mathrm{d}\hat{t}}[\hat{u}_i] \, \mathrm{d}\Omega, \quad i = 1, 2, 3, \tag{9}$$

where $\boldsymbol{n}$ is the outward normal to Ω_s. Where rotational motions of the plug are possible there will also be an equation describing the conservation of angular momentum. Such motions will not be considered here.

The basic flow considered is that of a two-dimensional channel formed by flat plates $\hat{y} = \pm L$ with an imposed dimensional pressure gradient P_0 in the $\hat{x}$-direction, i.e.

$$\hat{p} = -P_0 \hat{x} \tag{10}$$

(with an appropriate choice of coordinate origin). In this configuration there exists a steady 'Poiseuille flow' solution, $\hat{\boldsymbol{u}} = (\hat{U}(\hat{y}), 0, 0)$. By considering a parallelepiped of fluid, of width $2\hat{y}$, centred in the channel, one finds that the only non-zero component of $\hat{\boldsymbol{\tau}}$ satisfies

$$\hat{\tau}_{12} = -P_0 \hat{y}. \tag{11}$$

At the channel wall, $\hat{\tau} = \tau_w \equiv LP_0$. If $\tau_0 < \tau_w$ then the yield stress will be exceeded for $|\hat{y}| > L\tau_0/\tau_w$ and the fluid will flow in the channel.

For $|\hat{y}| > L\tau_0/\tau_w$, the velocity component $\hat{U}(\hat{y})$ in the $\hat{x}$-direction satisfies

$$\frac{\mathrm{d}^2\hat{U}}{\mathrm{d}\hat{y}^2} = -\frac{P_0}{\mu_0}, \quad |\hat{y}| \geqslant L\frac{\tau_0}{\tau_w}, \tag{12}$$

with boundary conditions

$$\hat{U}(\pm L) = 0, \tag{13}$$

$$\frac{\mathrm{d}\hat{U}}{\mathrm{d}\hat{y}}\left(\pm L\frac{\tau_0}{\tau_w}\right) = 0. \tag{14}$$

In the region $|\hat{y}| < L\tau_0/\tau_w$ the yield stress is not exceeded, and from (1) the plug velocity satisfies

$$\frac{\mathrm{d}\hat{U}}{\mathrm{d}\hat{y}} = 0, \quad |\hat{y}| < L\frac{\tau_0}{\tau_w}. \tag{15}$$

The function $\hat{U}(\hat{y})$ that satisfies (12), (13), (14) and (15) is given by

$$\hat{U}(\hat{y}) = \begin{cases} \dfrac{L\tau_w}{2\mu_0}\left(1 - \dfrac{\tau_0}{\tau_w}\right)^2, & 0 \leqslant |\hat{y}| < L\dfrac{\tau_0}{\tau_w}, \\ \dfrac{L\tau_w}{2\mu_0}\left[\left(1 - \dfrac{\tau_0}{\tau_w}\right)^2 - \left(\dfrac{|\hat{y}|}{L} - \dfrac{\tau_0}{\tau_w}\right)^2\right], & L\dfrac{\tau_0}{\tau_w} \leqslant |\hat{y}| \leqslant L. \end{cases} \tag{16}$$

It is sketched in figure 1.

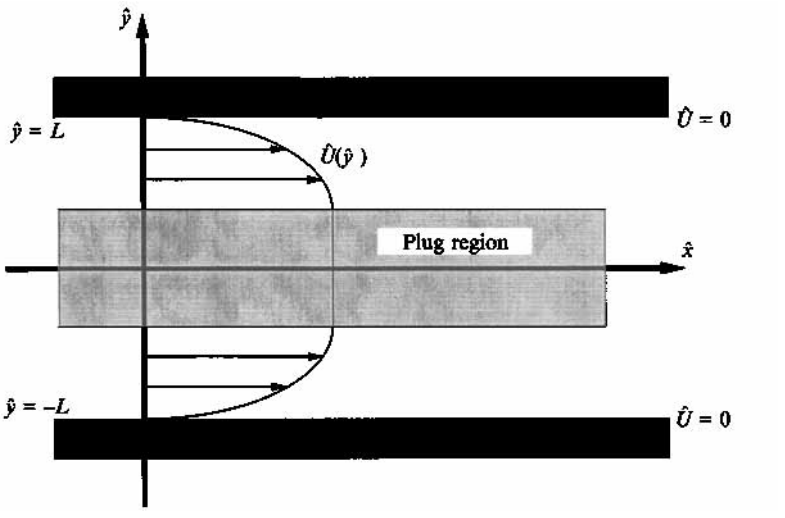

FIGURE 1. Poiseuille flow geometry and velocity profile for a Bingham fluid

These equations are non-dimensionalized using a lengthscale L, a velocity scale

$$U_0 = \frac{L\tau_w}{2\mu_0}\left(1 - \frac{\tau_0}{\tau_w}\right)^2. \tag{17}$$

and a stress/pressure scale ρU_0^2. Two non-dimensional groups are defined: a Reynolds number

$$R = \rho U_0 L/\mu_0, \tag{18}$$

and a Bingham number

$$B = \frac{\tau_0 L}{\mu_0 U_0}\left[= \frac{2\tau_0/\tau_w}{(1-\tau_0/\tau_w)^2}\right]. \tag{19}$$

Using this non-dimensionalization, and omitting the hat notation for dimensionless variables, the full equations of motion are

$$\nabla \cdot \boldsymbol{u} = 0, \tag{20}$$

$$\boldsymbol{u}_t + (\boldsymbol{u}\cdot\nabla)\boldsymbol{u} = \nabla\cdot(-p\boldsymbol{\delta} + \boldsymbol{\tau}), \tag{21}$$

$$\boldsymbol{\tau} = \frac{1}{R}\eta(\dot{\gamma})\dot{\boldsymbol{\gamma}} \Leftrightarrow \tau \geqslant \frac{B}{R}, \tag{22}$$

$$\dot{\gamma} = 0 \Leftrightarrow \tau < B/R, \tag{23}$$

$$\eta(\dot{\gamma}) = 1 + B/\dot{\gamma}, \tag{24}$$

$$\oint_{\partial\Omega_s} \sigma_{i,j} n_j \,\mathrm{d}s = \int_{\Omega_s} \frac{\mathrm{d}}{\mathrm{d}t}[u_i]\,\mathrm{d}\Omega, \quad i = 1, 2, 3. \tag{25}$$

The usual form of the Navier–Stokes equations for a Newtonian fluid is recovered when $B = 0$. After scaling, the basic Poiseuille flow solution, $(p, \boldsymbol{u}) = (P, \boldsymbol{U}) = (P(x), U(y), 0, 0)$, becomes

$$P(x) = -\frac{B\tau_w}{R\tau_0}x, \tag{26}$$

$$U(y) = \begin{cases} 1, & 0 \leqslant |y| < \dfrac{\tau_0}{\tau_w}, \\ 1 - \left(\dfrac{|y| - \tau_0/\tau_w}{1-\tau_0/\tau_w}\right)^2, & \dfrac{\tau_0}{\tau_w} \leqslant |y| \leqslant 1. \end{cases} \tag{27}$$

Before analysing the linear stability of this solution to two-dimensional perturbations in the next section, the unsteady one-dimensional case of (20)–(25), in which all quantities are independent of x, is briefly considered.

Assume symmetry about $y = 0$ and suppose that at $t = 0$ the yield surface is at $y = s_0 \mp \tau_0/\tau_w$. Then in the evolution towards the steady solution (27), the unsteady horizontal velocity $u(y, t)$ and yield surface $s(t)$ satisfy

$$\frac{\partial u}{\partial t} = \frac{B\tau_w}{R\tau_0} + \frac{1}{R}\frac{\partial^2 u}{\partial y^2}, \quad s(t) < y < 1, \tag{28}$$

with initial and boundary conditions

$$u(y, 0) = u_0(y), \tag{29}$$

$$u(1, t) = 0, \tag{30}$$

$$u(s(t), t) = u_s(t), \tag{31}$$

$$\frac{\partial u}{\partial y}(s(t), t) = 0. \tag{32}$$

The equation of motion of the plug, with speed $u_s(t)$, is given by

$$s(t)\frac{\mathrm{d}u_s}{\mathrm{d}t} = \frac{B\tau_w}{R\tau_0}s(t) - \frac{B}{R}. \tag{33}$$

The first term on the right-hand side of (33) is the action of the pressure gradient and the second term is the action of the shear stress (equal to the yield stress, B/R); the left-hand side is the acceleration of the material in the plug region.

This problem is stated here for two reasons. First, it is the simplest stability problem for a Poiseuille flow of a Bingham fluid and, as such, illustrates straightforwardly the main flow parameters. This problem has been studied extensively by Comparini (1992), who proves existence and uniqueness of a solution. The linear stability of the steady solution to (28)–(33) is considered in the next section, along with the two-dimensional analysis. Secondly, (31)–(33) illustrate very clearly the interpretation of Bingham fluid flow problems as free boundary problems.

Whilst free boundaries are often found in fluid instability problems, the free boundaries commonly represent material surfaces. For a Bingham fluid this is not the case, since the yield surface is *not* a material surface (i.e. the left-hand side of (33) is not $(\mathrm{d}/\mathrm{d}t)[s(t)u_s(t)]$). For this reason Bingham fluid flow problems often resemble other (non-fluid dynamical) free boundary problems. Such an analogy can at times be helpful. In fact, by setting $\theta = u_y$ and eliminating u_s in the above, one obtains a free boundary problem for θ that is very closely related to the classical Stefan problem, for phase change in a pure material; see e.g. Comparini (1992).

3. Linear stability analysis

Consider an infinitesimal disturbance of form $(\epsilon p, \epsilon \boldsymbol{u})$, where $\epsilon \ll 1$, to the primary flow (P, U) described by (26) and (27) above. The perturbed flow satisfies

$$\nabla \cdot [U + \epsilon \boldsymbol{u}] = 0, \tag{34}$$

$$\epsilon \boldsymbol{u}_t + [(U + \epsilon \boldsymbol{u}) \cdot \nabla][U + \epsilon \boldsymbol{u}] = \nabla \cdot \boldsymbol{\sigma}(P + \epsilon p, U + \epsilon \boldsymbol{u}). \tag{35}$$

Wherever the yield stress is exceeded, the effective viscosity of the perturbed flow is expanded about the basic flow, i.e.

$$\eta(\boldsymbol{U}+\epsilon\boldsymbol{u}) = \eta(\boldsymbol{U}) + \epsilon\dot{\gamma}_{ij}(\boldsymbol{u})\frac{\partial\eta}{\partial\dot{\gamma}_{ij}}(\boldsymbol{U}) + O(\epsilon^2). \tag{36}$$

Linearized disturbance equations are derived by substitution of (36) into (35) and subtraction of the primary flow equations, retaining terms of order ϵ only. These equations are

$$\nabla\cdot\boldsymbol{u} = 0, \tag{37}$$

$$u_t + vU_y + Uu_x = -p_x + \frac{1}{R}\nabla^2 u + \frac{B}{R}\left\{\frac{\nabla^2 u - u_{yy} - v_{ux}}{\dot{\gamma}(U)}\right\}, \tag{38}$$

$$v_t + Uv_x = -p_y + \frac{1}{R}\nabla^2 v + \frac{B}{R}\left\{2v_y\frac{\mathrm{d}}{\mathrm{d}y}\left[\frac{1}{\dot{\gamma}(U)}\right] + \frac{\nabla^2 v - v_{xx} - u_{yx}}{\dot{\gamma}(U)}\right\}, \tag{39}$$

$$w_t + Uw_x = -p_z + \frac{1}{R}\nabla^2 w + \frac{B}{R}\left\{(v_z + w_y)\frac{\mathrm{d}}{\mathrm{d}y}\left[\frac{1}{\dot{\gamma}(U)}\right] + \frac{\nabla^2 w}{\dot{\gamma}(U)}\right\}. \tag{40}$$

Equations (37)–(40) describe the evolution of the velocity and pressure perturbations from arbitrary initial conditions, given appropriate linearized boundary conditions.

At the fixed boundaries of the flow region it follows from the no-slip condition that

$$\boldsymbol{u} = 0 \quad \text{on} \quad y = \pm 1. \tag{41}$$

This is sufficient to describe the linear stability problem for a Newtonian fluid, $B = 0$. For $B > 0$, it is assumed that the yield surfaces at $y = \pm\tau_0/\tau_w$ undergo an initially smooth perturbation of size $O(\epsilon)$, during which the plug persists, and that any instability then develops from this initial perturbation.

Some justification for this assumption comes from the observation that a Bingham fluid models a real fluid which behaves both as a viscous fluid and as an elastic solid, depending on whether or not a certain yield stress is exceeded. Since an elastic solid would not break up, it is a physically desirable property of the model that the solid plug should also be able to withstand an infinitesimal perturbation without breaking up. Further discussion may be found in Frigaard (1990).

The perturbation $(\epsilon p, \epsilon\boldsymbol{u})$ is assumed periodic in the x- and z-directions, say with periods $2X$ and $2Z$ respectively. The yield surfaces at $y = \pm\tau_0/\tau_w$ perturb to

$$y = \pm\tau_0/\tau_w \pm \epsilon h_{\pm}(x, z, t), \tag{42}$$

where h_+ and h_- are also assumed periodic in x and z. The yield criterion (8) is linearized about the continuation into the plug region of the primary 'fluid' velocity field. Equation (25) is also linearized about the basic flow. These linearizations involve the yield surface perturbations, $\epsilon h_{\pm}$, as well as the pressure and velocity perturbations. The boundary conditions at the yield surfaces become

$$u_x(x, \pm\tau_0/\tau_w, z, t) = 0, \tag{43}$$

$$v_y(x, \pm\tau_0/\tau_w, z, t) = 0, \tag{44}$$

$$w_z(x, \pm\tau_0/\tau_w, z, t) = 0, \tag{45}$$

$$u_z(x, \pm\tau_0/\tau_w, z, t) + w_x(x, \pm\tau_0/\tau_w, z, t) = 0, \tag{46}$$

$$w_y(x, \pm\tau_0/\tau_w, z, t) + v_z(x, \pm\tau_0/\tau_w, z, t) = 0, \tag{47}$$

$$v_x(x, \pm\tau_0/\tau_w, z, t) + u_y(x, \pm\tau_0/\tau_w, z, t) = \frac{\pm 2h_{\pm}(x, z, t)}{(1-\tau_0/\tau_w)^2}, \tag{48}$$

and $$u_t(x, \pm\tau_0/\tau_w, t) = \frac{B\tau_w^2}{R\tau_0^2}\frac{1}{8XZ}\int_{-X}^{X}\int_{-Z}^{Z}[h_+(x,z,t)+h_-(x,z,t)]\,dx\,dz, \tag{49}$$

$$v_t(x, \pm\tau_0/\tau_w, t) = \frac{\tau_w}{\tau_0}\frac{1}{8XZ}\int_{-X}^{X}\int_{-Z}^{Z}[p(x, -\tau_0/\tau_w, z, t)-p(x, \tau_0/\tau_w, z, t)]\,dx\,dz, \tag{50}$$

$$w_t(x, \pm\tau_0/\tau_w, t) = 0. \tag{51}$$

Derivation of these equations is described in detail in an Appendix at the end of the paper.

3.1. *One-dimensional perturbations*

Linear stability of plane Poiseuille flow of a Bingham fluid is determined by the behaviour of solutions to (37)–(40), subject to the boundary conditions (41), conditions of periodicity at $x = \pm X$, $z = \pm Z$, and the conditions (43)–(51) at $y = \pm\tau_0/\tau_w$. The disturbance equations and boundary conditions are linear. Substitution of an expansion of the solution in terms of normal modes yields an eigenvalue problem. Periodicity of the solution in the x- and z-directions suggests that the one-dimensional case

$$(p, \boldsymbol{u}, h_\pm) \sim (p(y), u(y), v(y), w(y), h_+, h_-)\,e^{\lambda t} \tag{52}$$

is special, since for all other normal modes the integrals involved in (49) and (50) integrate to zero. The normal mode (52) corresponds to a straightforward expansioin or contraction of the plug region.

On substituting (52) into the linear disturbance equations and boundary conditions, it is easily found that $v(y) = 0$, $w(y) = 0$ and $p(y) = \text{constant}$. There remains the following problem for $u(y)$ and $h_\pm$ (compare with (28)–(33)):

$$u_{yy}(y) - \lambda R u(y) = 0, \quad \frac{\tau_0}{\tau_w} < |y| < 1, \tag{53}$$

$$u_y \mp \frac{2h_\pm}{(1-\tau_0/\tau_w)^2} = 0, \quad y = \pm\frac{\tau_0}{\tau_w}, \tag{54}$$

$$u - \frac{B\tau_w^2}{2\lambda R\tau_0^2}(h_+ + h_-) = 0, \quad y = \pm\frac{\tau_0}{\tau_w}, \tag{55}$$

$$u = 0, \qquad y = \pm 1. \tag{56}$$

On taking (55) and (56) as Dirichlet boundary conditions for u, it is seen that $u(y)$ and $u(-y)$ satisfy identical equations and boundary conditions for $|y| \in [\tau_0/\tau_w, 1]$. Thus, u is even, u_y is odd, and $h_+ = h_-$, from (54). It is sufficient only to consider $y > 0$. By setting

$$\beta^2 = \lambda R(1-\tau_0/\tau_w)^2,$$

$$y = \frac{\tau_0}{\tau_w} + \xi(1-\tau_0/\tau_w),$$

and eliminating $h_\pm$, the problem transforms to

$$u_{\xi\xi}(\xi) - \beta^2 u(\xi) = 0, \quad 0 < \xi < 1, \tag{57}$$

$$u_\xi - \tfrac{1}{2}\beta^2 B(1-\tau_0/\tau_w)\,u = 0, \quad \xi = 0, \tag{58}$$

$$u = 0, \quad \xi = 1. \tag{59}$$

Note that λ is real, since u is real. Hence, positive values of λ correspond to real β. Non-trivial solutions for u are of form $u(\xi) = A\sinh\beta(1-\xi)$, satisfying the boundary condition at $\xi = 1$. To satisfy the condition at $\xi = 0$, requires that

$$\beta\cosh\beta + \tfrac{1}{2}\beta^2 B(1-\tau_0/\tau_w)\sinh\beta = 0 \tag{60}$$

have a solution. It is easily verified that (60) has no real solutions for $\beta \neq 0$. Hence, the mode (52) is unconditionally linearly stable.

3.2. *Normal modes and the Orr–Sommerfeld equation*

For normal modes other than (52) the integrals in (49) and (50) vanish, but the eigenvalue problem becomes multi-dimensional. For simplicity, only two-dimensional perturbations are considered. It can be seen from (38)–(40) that the coupling between the x- and y-direction velocity perturbations is much stronger than with that in the z-direction. Indeed, when there is no pressure perturbation p, (38) and (39) uncouple completely and could be considered separately. With a Newtonian fluid ($B = 0$) Squire's transformation guarantees that, as R is increased from zero, a planar Poiseuille flow will first become unstable to infinitesimal disturbances which are two-dimensional (Squire 1933). When $B > 0$ Squire's transformation cannot be applied and instead it will be assumed that the flow first becomes unstable to two-dimensional disturbances.

For a two-dimensional perturbation the continuity equation (37) can be satisfied by use of a stream function $\Psi(x, y, t)$, setting

$$u = \Psi_y(x, y, t), \quad v = -\Psi_x(x, y, t).$$

In normal mode form the solution may be written as

$$(\Psi, p, h_\pm) = (f(y), p(y), h_\pm)\,\mathrm{e}^{\mathrm{i}\alpha(x-ct)}.$$

Since $\alpha = 0$ has been considered above, only $\alpha > 0$ is considered. On taking the curl of (38) and (39), and substituting in a normal mode, after a little algebra one gets

$$\mathrm{i}\alpha R[(U-c)(f_{yy}-\alpha^2 f) - fU_{yy}] = \left[\frac{\mathrm{d}^2}{\mathrm{d}y^2} - \alpha^2\right]^2 f - 4\alpha^2 B\frac{\mathrm{d}}{\mathrm{d}y}\left[\frac{f_y}{|U_y|}\right]. \tag{61}$$

This is the Orr–Sommerfeld equation for a Bingham fluid. It is a fourth-order ordinary differential equation for $f(y)$, $|y| \in (\tau_0/\tau_w, 1)$, and may be seen to reduce to its more familiar form for a Newtonian fluid by letting $B \to 0$. For different R, B, τ_0/τ_w and α, this becomes an eigenvalue problem for c. Positive values of $\mathrm{Im}\,(c)$ correspond to unstable normal modes. Boundary conditions at $y = \pm 1$ are that

$$f = 0, \tag{62}$$

$$f_y = 0, \tag{63}$$

and at $y = \pm\tau_0/\tau_w$, from (43)–(50),

$$f_y = 0, \tag{64}$$

$$f_{yy} - \alpha^2 f = \pm\frac{2h_\pm}{(1-\tau_0/\tau_w)^2}, \tag{65}$$

$$f = 0. \tag{66}$$

Since (61) is symmetric about $y = 0$, the problems in the two fluid regions clearly

uncouple and are equivalent. Hence, it is sufficient to consider only one region, say $y \in [\tau_0/\tau_w, 1]$. By putting $y = \tau_0/\tau_w + \xi(1-\tau_0/\tau_w)$, and defining

$$\tilde{R} = (1-\tau_0/\tau_w)\,R, \tag{67}$$

$$\tilde{B} = (1-\tau_0/\tau_w)\,R, \tag{68}$$

$$\tilde{\alpha} = (1-\tau_0/\tau_w)\,\alpha, \tag{69}$$

(61) transforms into

$$\mathrm{i}\tilde{\alpha}\tilde{R}[(1-\xi^2-c)(f''(\xi)-\tilde{\alpha}^2 f)+2f(\xi)] = \left(\frac{\mathrm{d}^2}{\mathrm{d}\xi^2}-\tilde{\alpha}^2\right)\left(\frac{\mathrm{d}^2}{\mathrm{d}\xi^2}-\tilde{\alpha}^2\right)f(\xi) - 4\tilde{\alpha}^2\tilde{B}\frac{\mathrm{d}}{\mathrm{d}\xi}\left[\frac{f'(\xi)}{2|\xi|}\right], \tag{70}$$

where a prime denotes differentiation with respect to ξ. The non-dimensional numbers $\tilde{R}$ and $\tilde{B}$ will be called the *reduced* Reynolds and Bingham numbers for this problem, since they use the width of the yielded flow region in the primary flow as an appropriate lengthscale instead of the half-channel width. The definition of $\tilde{\alpha}$ then amounts to measuring the wavelengths of the normal modes in terms of the new lengthscale. Now $\xi \in [0, 1]$ and the boundary conditions become

$$f(1) = f'(1) = 0, \tag{71}$$

$$f(0) = f'(0) = 0, \tag{72}$$

$$f''(0) = 2h. \tag{73}$$

The last of these ensures that

$$f'/2\xi \to h \quad \text{as} \quad \xi \to 0.$$

4. Numerical solution of the Orr–Sommerfeld equation

Equation (70) and the boundary conditions (71), (72), and (73) constitute an eigenvalue problem for the complex eigenvalue c. It is of interest to determine the curves of marginal stability in the $(\tilde{\alpha}, \tilde{R})$-plane, i.e. those curves on which $\mathrm{Im}(c) = 0$.

Asymptotic methods might be used for very large $\tilde{R}$; indeed it is not hard to see that as $\tilde{R} \to \infty$ for each fixed $\tilde{B}$, the marginal stability curves will approach the Newtonian marginal stability curve asymptotically. To determine the marginal stability curves closer to the minimum critical reduced Reynolds numbers, numerical solution will be more accurate. A number of different numerical methods are available, each with their own advantages.

A sensible approach is to start with the marginal stability curve for a Newtonian flow, and then 'track' points on this curve as $\tilde{B}$ is increased from zero. The Riccati method was used for this purpose. This method transforms the Orr–Sommerfeld equation into four first-order nonlinear ordinary differential equations, and in doing so exchanges the eigenvalue problem for the equivalent problem of determining values of $\tilde{R}$, $\tilde{\alpha}$ and $\mathrm{Re}(c)$ for which the boundary conditions are satisfied at the correct 'characteristic length', ($\mathrm{Im}(c) \equiv 0$, $\tilde{B}$ fixed). For consistency with the Newtonian results on the stability of plane Poiseuille flow, only the case where f extends to an even function of ξ over $[-1, 1]$ is considered.† For the Newtonian problem, it is these eigenfunctions that are found to be unstable.

† If f is odd then $f''''(0) = 0$, and from (72) and (73) it follows that $f(0) = f'(0) = f''(0) = 0$. Since also (70) must be satisfied at $\xi = 0$,

$$\lim_{\xi \to 0}[f'(\xi)/\xi^2] = 0.$$

Thus, $f'''(\xi) \to 0$ as $\xi \to 0$, and successive derivatives of f at $\xi = 0$ are also equal to zero, by differentiating (70); expanding f about $\xi = 0$ implies $f \equiv 0$.

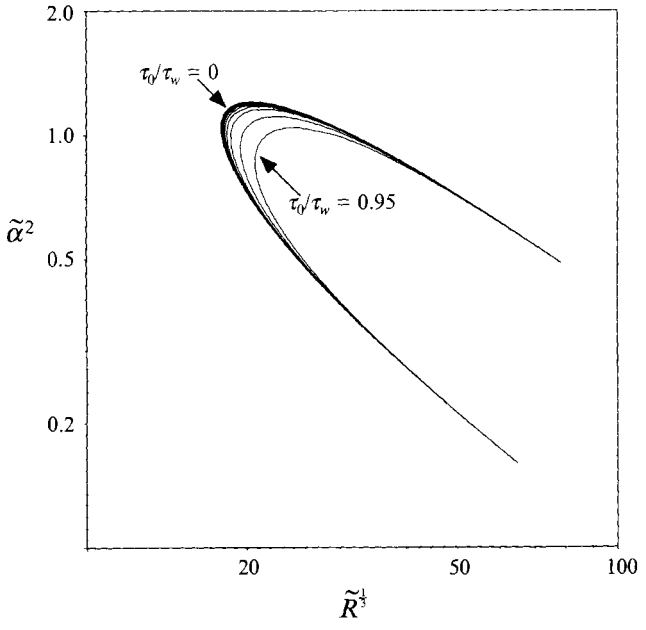

FIGURE 2. Marginal stability curves for $\tau_0/\tau_w \in [0, 1]$.

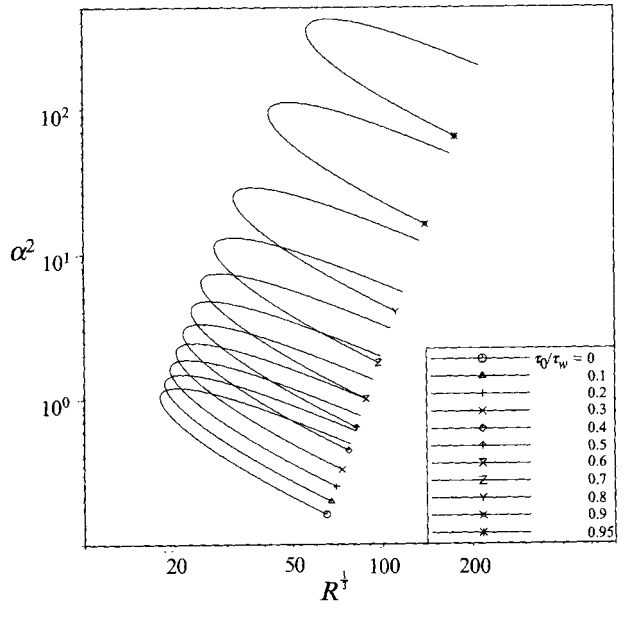

FIGURE 3. Marginal stability curves for $\tau_0/\tau_w \in [0, 1]$.

The Riccati method has been applied to the Newtonian problem by both Davey (1977) and Sloan (1977). The main advantages of using this method are that the forward integration of the transformed system has been found to be stable (which is not the case for more standard shooting methods), and that the method allows simple computation of the eigenfunctions as well as the eigenvalues. A complete introduction to the method may be found in Scott (1973), with extensions and applications in Davey (1977), Sloan (1977), Sloan & Wilks (1976), Wilks & Sloan (1976). Use of the Riccati

τ_0/τ_w	B	$\tilde{B}$	$\tilde{R}_c$	R_c	c_R	$\tilde{\alpha}$
0	0	0	5772.22	5772.22	0.264000	1.020550
0.10	0.2	0.2	5795.26	6439.17	0.263701	1.019650
0.20	0.6	0.5	5823.94	7279.92	0.263336	1.018580
0.30	1.2	0.9	5860.63	8372.32	0.262862	1.017140
0.40	2.2	1.3	5909.23	9848.72	0.262246	1.015310
0.50	4.0	2.0	5976.70	11953.41	0.261399	1.012780
0.60	7.5	3.0	6076.70	15191.74	0.260168	1.009120
0.70	15.6	4.7	6240.33	20801.09	0.258207	1.003300
0.80	40.0	8.0	6557.47	32787.37	0.254582	0.992572
0.90	180.0	18.0	7445.55	74455.48	0.245504	0.965959
0.95	760.0	38.0	9034.60	180692.00	0.232240	0.927603

TABLE 1. Minimum critical conditions for instability to linearized two-dimensional disturbances. The first line, $\tau_0/\tau_w = 0$, are the values obtained by Orszag (1971).

method for this problem requires some minor modifications to deal with the singularity at $\xi = 0$. A full description of this application may be found in Frigaard (1990), where there is also some discussion of the accuracy and efficiency of the method.

The marginal stability curve for a Newtonian fluid was first computed starting at the critical values of $\tilde{R}$, $\tilde{\alpha}$ and $\mathrm{Re}(c)$ that were computed by Orszag (1971). Points on this curve were used as an initial approximation for points on the $\tilde{B} = \frac{2}{9}$ stability curve. Better approximations were found iteratively. The procedure was repeated for successively higher values of $\tilde{B}$. From these critical values of $\tilde{\alpha}$ and $\tilde{R}$, for each $\tilde{B}$ a marginal stability curve was constructed by interpolation. These curves are shown in figure 2, where $\tilde{R}^{\frac{1}{3}}$ has been plotted against $\tilde{\alpha}^2$ on logarithmic scales.

The Newtonian results are in very good agreement with previously computed results. The Bingham results appear to form a series of nested curves (with increasing reduced Bingham number, or $\tilde{B}$) inside the Newtonian curve. Greater clarity is achieved by plotting $R^{\frac{1}{3}}$ against α^2 on logarithmic scales, when the marginal stability curves separate out; see figure 3. Figures 2 and 3 show clearly the stabilizing effect of an increasing yield stress on the flow. Not only are higher Reynolds numbers required for instability as $\tilde{B}$ increases, but the flow is also unstable only to disturbances with wavelengths that lie within a range that becomes successively shorter as $\tilde{B}$ increases.

Using points on these curves as starting points, each marginal stability curve was tracked until a minimum critical Reynolds number was reached for each value of $\tilde{B}$. The computed critical parameter values are contained in table 1. From table 1, the critical minimum Reynolds number for linear instability, $\tilde{R}_c$, was plotted against $\tilde{B}$, and also R_c was plotted against B, see figure 4(a, b). The relationship between $\tilde{R}_c$ and $\tilde{B}$ appears to be almost linear (figure 4a).

For the minimum critical Reynolds numbers in table 1, the eigenfunctions were also computed for various $\tilde{B}$. The real and imaginary parts of these are plotted in figure 5, from 100 evenly spaced points in $[0, 1]$. Values at $\xi = 0.1 \times k$, $k = 0, \ldots, 10$ for the Newtonian flow, $\tilde{B} = 0$, agree exactly with those computed by Sloan (1977). The Bingham results show a steady variation from the Newtonian results as $\tilde{B}$ increases from zero.

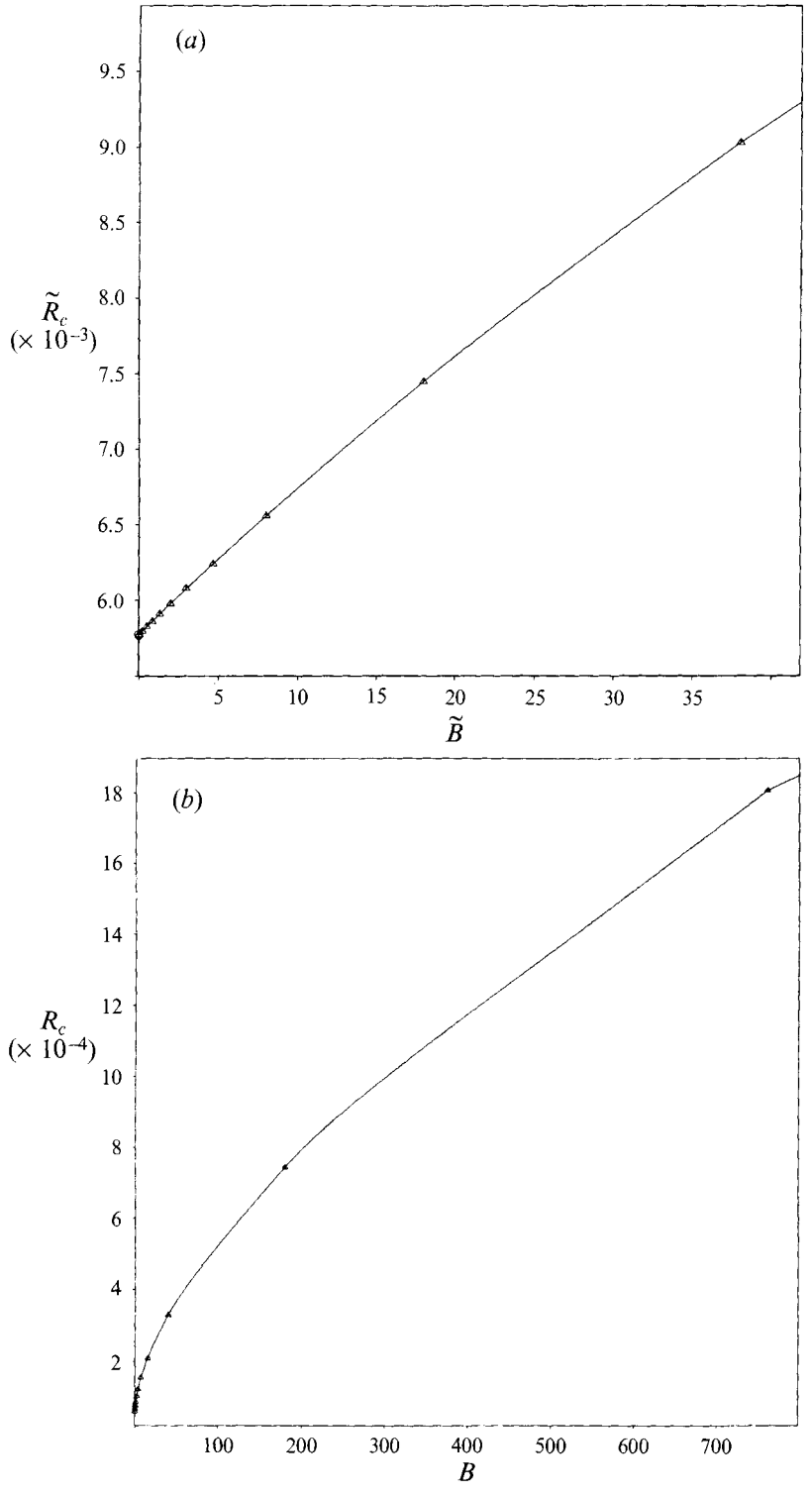

FIGURE 4. Variation in critical reduced Reynolds number with reduced Bingham number. ○, Orszag's value at $B = 0$.

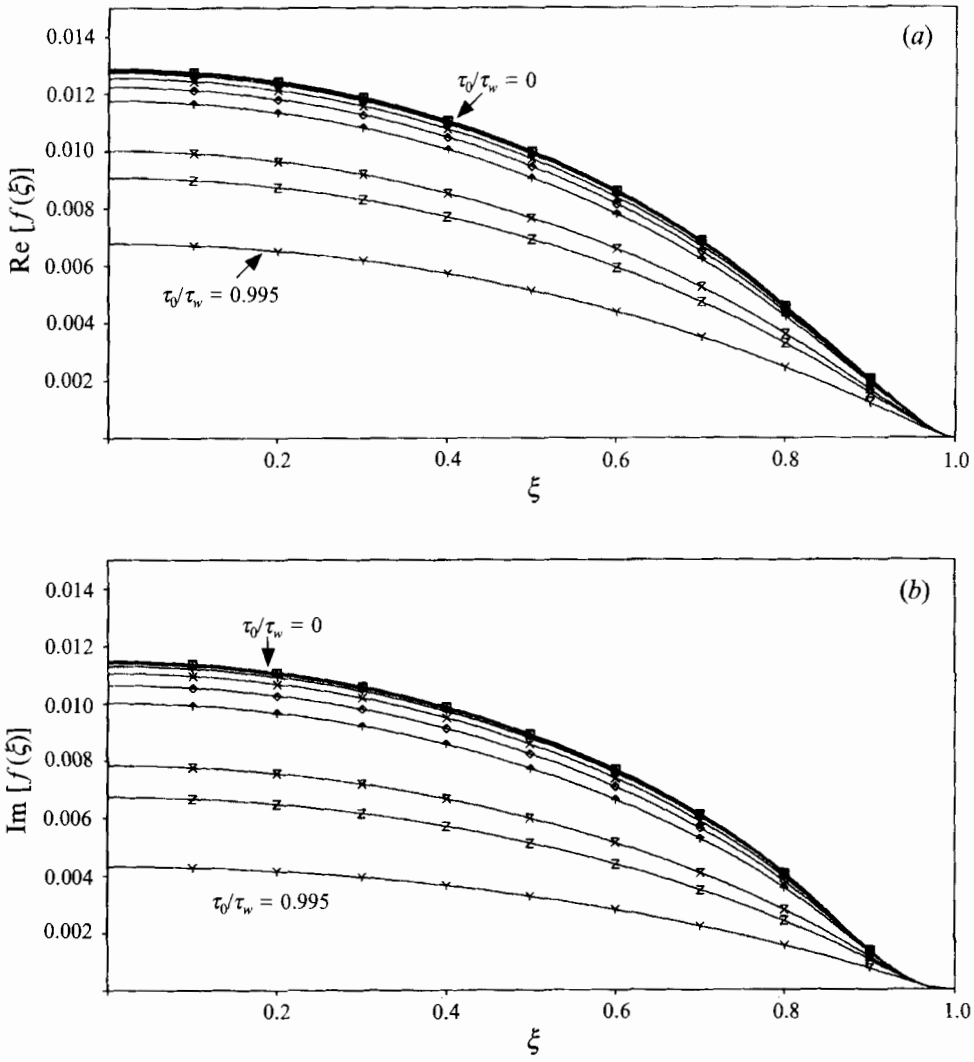

FIGURE 5. Variation in eigenfunctions at critical Reynolds number with τ_0/τ_w.

5. Discussion and conclusions

Only the simplest stability problem for a Bingham fluid has been considered. The results show that there is a significant increase in the critical Reynolds number for two-dimensional, linear instability as the yield stress increases. In comparison with Pratt's experimental results, the results presented here show that transition is subcritical in Poiseuille flow of a Bingham fluid.

In typical drilling situations the Bingham number might vary between 10 and 100, for which R_c can increase by an order of magnitude. Suppose that instead of the limiting viscosity μ_0, one uses an effective viscosity scale to define a Reynolds number R_e, i.e.

$$R_e = \rho L_e U_e / \eta_e,$$

where L_e, U_e and η_e are the chosen lengthscale, velocity scale and effective viscosity scale, respectively. Transitional Reynolds numbers defined in this way do not show

much variation with the yield stress. Thus, assume that for a Bingham channel flow transition takes place at $R_e = R_e^* \approx C_1$. The effective viscosity scale, η_e, has the form

$$\eta_e = \mu_0 + C_2 \tau_0 L_e / U_e.$$

Assuming a linear relationship among L_e, U_e and L, U_0 used in §2, this then implies that the transitional Reynolds number, R^*, defined using the limiting viscosity μ_0, satisfies

$$R^* \approx \tilde{C}_1 + \tilde{C}_2 B.$$

Thus, the experimental finding of there being little variation in R_e^* implies an approximately linear variation in R^* with B. This parallels the linear increase in $\tilde{R}_c$ with $\tilde{B}$, shown in figure 4(*a*). However, it is clear that the growth rates of $\tilde{R}_c$ with $\tilde{B}$ and of R^* with B are very different.

Alternatively, one can compare the observed growth in R^* with B and the computed growth in R_c with B. Although the computed and observed increases are of simnilar order of magnitude, the growth rates are once again very different (e.g. $B = 0$, $R_c \approx 5772$, $R^* \approx 1000$; $B = 0.45$, $R_c \approx 7000$, $R^* \approx 1400$; $B = 560$, $R_c \approx 145000$, $R^* \approx 26700$).

Viscosity plays a dual role in fluid instability. On the other hand, by definition, viscosity helps to dissipate energy internally within the fluid. However, on the other hand, this same dissipation allows the diffusive transfer of energy from the unperturbed flow to the perturbation. For $B = 0$, Newtonian transition to turbulence in plane Poiseuille flows occurs rapidly, on the convective timescale of the unperturbed flow. Maximum growth rates of the unstable two-dimensional, linear Orr–Sommerfeld modes are much slower, and are essentially diffusive. This partly explains the discrepancy between R^* and R_c, at $B = 0$.

For $B > 0$ the convective timescale remains the same non-dimensionally, but diffusive/dissipative timescales become much shorter, owing to the increased viscosity. Note that $\eta \to \infty$ at a yield surface and that R^{-1} characterized only the limiting non-dimensional viscosity, at high rates of strain. Thus, although the results do indicate increasing flow stability with B (i.e. since R_c increases), it is quite possible that the maximum growth rates of unstable Orr–Sommerfeld modes also increase with B. This computationally intensive investigation has not been undertaken.

Appendix. Linearized boundary conditions at the yield surfaces

A complete derivation of the linear yield surface boundary conditions, (43)–(48) and (49)–(51), is given here.

First, the yield criterion and continuity of stress throughout the fluid demand that $\dot{\gamma}(\boldsymbol{U} + \epsilon \boldsymbol{u}) = 0$ at each perturbed yield surface. This implies that

$$\dot{\gamma}_{ij}(\boldsymbol{U} + \epsilon \boldsymbol{u}) = 0, \quad y = \pm \tau_0/\tau_w \pm \epsilon h_\pm, \quad i,j = 1,2,3. \tag{A 1}$$

By writing

$$\boldsymbol{u}(x, \pm \tau_0/\tau_w \pm \epsilon h_\pm, z, t) = \boldsymbol{u}(x, \pm \tau_0/\tau_w, z, t) + O(\epsilon),$$

and continuing the primary 'fluid' velocity into the plug region, where necessary, i.e.

$$U(\pm \tau_0/\tau_w \pm \epsilon h_\pm) = \frac{\mp 2\epsilon h_\pm}{(1 - \tau_0/\tau_w)^2},$$

the conditions (43)–(48) follow directly from (A 1).

Secondly, the momentum condition on the plug, (25), must be linearized to give (49)–(51). For a periodic perturbation as described, let Ω_s denote that part of the plug for which $(x, z) \in [-X, X] \times [-Z, Z]$. Equation (25) for the perturbed flow is

$$\oint_{\partial\Omega_s} \sigma_{ij}(P+\epsilon p, U+\epsilon u)\, n_j \,\mathrm{d}s = \int_{-X}^{X}\int_{-Z}^{Z}\int_{-\tau_0/\tau_w-\epsilon h_-}^{\tau_0/\tau_w+\epsilon h_+} \epsilon \frac{\mathrm{d}}{\mathrm{d}t} u_i \,\mathrm{d}x. \tag{A 2}$$

To leading order the right-hand side of (A 2) straightforwardly becomes

$$\int_{-X}^{X}\int_{-Z}^{Z}\int_{-\tau_0/\tau_w-\epsilon h_-}^{\tau_0/\tau_w+\epsilon h_+} \epsilon \frac{\mathrm{d}}{\mathrm{d}t} u_i \,\mathrm{d}x = \frac{8\epsilon XZ\tau_0}{\tau_w} \frac{\partial}{\partial t} u_i\left(x, \pm\frac{\tau_0}{\tau_w}, z, t\right) + O(\epsilon^2). \tag{A 3}$$

For the left-hand side of (A 2), subtraction of

$$\frac{\partial}{\partial x_j}\sigma_{ij}(P, U) \equiv 0$$

and use of the divergence theorem produces

$$\oint_{\partial\Omega_s} \sigma_{ij}(P+\epsilon p, U+\epsilon u)\, n_j \,\mathrm{d}s = \oint_{\partial\Omega_s} [-\epsilon p\delta_{ij} + \tau_{ij}(U+\epsilon u) - \tau_{ij}(U)]\, n_j \,\mathrm{d}s. \tag{A 4}$$

The surface integrals in (A 4) at $x = \pm X$ and $z = \pm Z$ will cancel, due to the periodicity of p, u and $h_\pm$. This leaves only the surface integrals over each of the perturbed yield surfaces. On $y = \pm\tau_0/\tau_w \pm \epsilon h_\pm$, the outward surface normal vector, n, is given approximately by

$$n = \left(\epsilon\frac{\partial h_\pm}{\partial x}, \pm 1, \epsilon\frac{\partial h_\pm}{\partial z}\right) + O(\epsilon^2). \tag{A 5}$$

Since τ depends continuously on the fluid velocity, the right-hand side of (A 4) is $O(\epsilon)$. Substituting for n in (A 4), the left-hand side of (A 2) becomes

$$\begin{aligned}\oint_{\partial\Omega_s} \sigma_{ij}(P+\epsilon p, U+\epsilon u)\, n_j \,\mathrm{d}s = &\int_{-X}^{X}\int_{-Z}^{Z} [-\epsilon p\delta_{i2} + \tau_{i2}(U+\epsilon u) \\ &- \tau_{i2}(U)]\big|_{y=\tau_0/\tau_w+\epsilon h_+} \mathrm{d}z\,\mathrm{d}x \\ &- \int_{-X}^{X}\int_{-Z}^{Z} [-\epsilon p\delta_{i2} + \tau_{i2}(U+\epsilon u) \\ &- \tau_{i2}(U)]\big|_{y=-\tau_0/\tau_w-\epsilon h_-} \mathrm{d}z\,\mathrm{d}x + O(\epsilon^2).\end{aligned} \tag{A 6}$$

To evaluate the leading-order terms in the right-hand side of (A 6), the deviatoric stress is written as

$$\tau_{ij} = \tau_{ij}^Y + \tau_{ij}^E, \tag{A 7}$$

where

$$\tau_{ij}^Y \equiv (B/R\dot\gamma)\,\dot\gamma_{ij}, \tag{A 8}$$

$$\tau_{ij}^E \equiv (\dot\gamma_{ij}/R). \tag{A 9}$$

Both tensors τ_{ij}^Y and τ_{ij}^E are symmetric; τ_{ij}^Y is characterized by the fact that $\tau^Y = B/R$ always, whereas τ^E measures the variation from the yield stress. The terms $\tau_{ij}(U+\epsilon u) - \tau_{ij}(U)$ in (A 6) can be written as

$$\tau_{ij}(U+\epsilon u) - \tau_{ij}(U) = [\tau_{ij}^E(U+\epsilon u) - \tau_{ij}^E(U)] + [\tau_{ij}^Y(U+\epsilon u) - \tau_{ij}^Y(U)]. \tag{A 10}$$

For the perturbed flow, $\tau_{ij}^E = 0$ at $y = \pm\tau_0/\tau_w \pm \epsilon h_\pm$. For the basic unperturbed flow only τ_{12} is non-zero, with $\tau_{12}^E(U)$ given by

$$\tau_{12}^E(U) = \mp \epsilon h_\pm B\tau_w/R\tau_0, \quad y = \pm\tau_0/\tau_w \pm \epsilon h_\pm. \tag{A 11}$$

These will be the only terms from the first square bracket of (A 10) that will appear to leading order in the right-hand side of (A 6).

For terms from the second square bracket of (A 10), one writes

$$\int_{-X}^{X}\int_{-Z}^{Z} [\tau_{i2}^Y(\boldsymbol{U}+\epsilon\boldsymbol{u}) - \tau_{i2}^Y(\boldsymbol{U})]\,|_{y=\pm\tau_0/\tau_w\pm\epsilon h_\pm}\,\mathrm{d}z\,\mathrm{d}x$$

$$= \lim_{y\to\pm\tau_0/\tau_w} \int_{-X}^{X}\int_{-Z}^{Z} \tau_{i2}^Y(\boldsymbol{U}+\epsilon\boldsymbol{u}) - \tau_{i2}^Y(\boldsymbol{U})\,\mathrm{d}z\,\mathrm{d}x + O(\epsilon^2). \tag{A 12}$$

Expanding $\tau_{ij}^Y(\boldsymbol{U}+\epsilon\boldsymbol{u})$ about the primary flow gives

$$\tau_{ij}^Y(\boldsymbol{U}+\epsilon\boldsymbol{u}) - \tau_{ij}^Y(\boldsymbol{U}) = \epsilon\frac{B}{R}\left(\frac{\dot\gamma_{ij}(\boldsymbol{u})}{\dot\gamma(\boldsymbol{U})} + 2\dot\gamma_{12}(\boldsymbol{u})\frac{\partial}{\partial\dot\gamma_{12}}[\dot\gamma^{-1}(\boldsymbol{U})]\,\dot\gamma_{ij}(\boldsymbol{U})\right) + O(\epsilon^2). \tag{A 13}$$

For $i,j = 1,2$ the $O(\epsilon)$ term above vanishes. For $i,j = 2,2$ the right-hand side of (A 12) becomes

$$\epsilon\frac{B}{R}\lim_{y\to\pm\tau_0/\tau_w}\left[\frac{1}{\dot\gamma(\boldsymbol{U})}\int_{-X}^{X}\int_{-Z}^{Z}\dot\gamma_{22}(\boldsymbol{u})\,\mathrm{d}z\,\mathrm{d}x\right] + O(\epsilon^2)$$

$$= -\epsilon\frac{B}{R}\lim_{y\to\pm\tau_0/\tau_w}\left[\frac{1}{\dot\gamma(\boldsymbol{U})}\int_{-X}^{X}\int_{-Z}^{Z}\dot\gamma_{11}(\boldsymbol{u}) + \dot\gamma_{33}(\boldsymbol{u})\,\mathrm{d}z\,\mathrm{d}x\right] + O(\epsilon^2)$$

$$= 0 + O(\epsilon^2), \tag{A 14}$$

since $\dot\gamma_{11}(\boldsymbol{u})$ and $\dot\gamma_{33}(\boldsymbol{u})$ integrate exactly and vanish, due to the periodicity of $\boldsymbol{u}$.

For $i,j = 3,2$ consider the linearized momentum equation for w, (40). Under the assumption that the velocity perturbation in the z-direction remains finite initially, it follows that

$$\lim_{y\to\pm\tau_0/\tau_w}\left[\dot\gamma_{23}(\boldsymbol{u})\frac{\partial}{\partial y}\eta(\boldsymbol{U})\right] = O(1),$$

and hence that

$$\lim_{y\to\pm\tau_0/\tau_w}\left[\frac{\dot\gamma_{23}(\boldsymbol{u})}{\dot\gamma(\boldsymbol{U})}\right] = 0.$$

Thus, all the terms of form $\tau_{i2}^Y(\boldsymbol{U}+\epsilon\boldsymbol{u}) - \tau_{i2}^Y(\boldsymbol{U})$ that appear in (A 6) are $O(\epsilon^2)$. Collecting together the only $O(\epsilon)$ terms that remain in (A 2) (i.e. (A 11) and the non-zero pressure term from $\delta_{i2}p$), leads directly to (49), (50) and (51).

REFERENCES

Beris, A. N., Tsamopoulos, J. A., Armstrong, R. C. & Brown, R. A. 1985 Creeping motion of a sphere through a Bingham plastic. *J. Fluid Mech.* **158**, 219–244.

Comparini, E. 1992 A one-dimensional Bingham flow. *J. Math. Anal. Appl.* **169**, 127–139.

Davey, A. 1977 On the numerical solution of difficult eigenvalue problems. *J. Comput. Phys.* **24**, 331–338.

Davies, S. J. & White, C. M. 1928 An experimental study of the flow of water pipes of rectangular section. *Proc. R. Soc. Lond.* A **119**, 92–107.

DOWELL SCHLUMBERGER 1985 Rheology and flow calculations. In *Cementing technology*, chap. 4. Dowell Schlumberger.

FRIGAARD, I. A. 1990 The stability of parallel flow of a generalized Bingham fluid. MSc thesis, Oxford University.

HANKS, R. W. 1963 The laminar-turbulent transition for fluids with a yield stress. *AIChE J.* **9**, 306–309.

HANKS, R. W. & DADIA, B. H. 1971 Theoretical analysis of the turbulent flow of non-Newtonian slurries in pipes. *AIChE J.* **17**, 554–557.

HANKS, R. W. & PRATT, D. R. 1967 On the flow of Bingham plastic slurries in pipes and between parallel plates. *Soc. Petrol. Engrs J.* **7**, 342–346.

HERBERT, T. 1976 Periodic secondary motions in a plane channel. In *Proc. 5th Intl Conf. Numerical Methods in Fluid Dynamics* (ed. A. I. Van de Vooren & P. J. Zandbergen). Lecture Notes in Physics, vol. 59, pp. 235–240. Springer.

OLDROYD, J. G. 1947 Two-dimensional plastic flow of a Bingham solid. *Proc. Camb. Phil. Soc.* **43**, 383–395.

ORSZAG, S. A. 1971 Accurate solution of the Orr–Sommerfeld stability equation. *J. Fluid Mech.* **50**, 689–703.

ORSZAG, S. A. & KELLS, L. C. 1980 Transition to turbulence in plane Poiseuille and plane Couette flow. *J. Fluid Mech.* **96**, 159–205.

ORSZAG, S. A. & PATERA, A. T. 1983 Secondary instability of wall bounded shear flows. *J. Fluid Mech.* **128**, 347–385.

PATEL, V. C. & HEAD, M. R. 1969 Some observations in skin friction and velocity profiles in fully developed pipe and channel flows. *J. Fluid Mech.* **38**, 181–201.

SCOTT, M. R. 1973 An initial value method for the eigenvalue problem for systems of ODE's. *J. Comput. Phys.* **12**, 334–347.

SLOAN, D. M. 1977 Eigenfunctions of systems of linear ODE's with separated boundary conditions using Riccati transformations. *J. Comput. Phys.* **24**, 320–330.

SLOAN, D. M. & WILKS, G. 1976 Riccati transformations for eigenvalues of systems of linear ODE's with separated boundary conditions. *J. Inst. Maths Applics.* **18**, 117–127.

SQUIRE, H. B. 1933 On the stability for three-dimensional disturbances of viscous fluid flow between parallel walls. *Proc. R. Soc. Lond.* A **142**, 621–628.

THOMAS, D. G. 1960 Heat and momentum transport characteristics of non-Newtonian aqueous thorium oxide suspensions. *AIChE J.* **6**, 631–639.

WALTON, I. C. & BITTLESTON, S. H. 1991 The axial flow of a Bingham plastic in a narrow annulus. *J. Fluid Mech.* **222**, 39–60.

WILKS, G. & SLOAN, D. M. 1976 Invariant imbedding, Riccati transformation and eigenvalue problems. *J. Inst. Maths Applics.* **18**, 99–116.

ZAHN, J. P., TOOMRE, J. SPIEGEL, E. A. & GOUGH, D. O. 1974 Nonlinear cellular motions in Poiseuille channel flow. *J. Fluid Mech.* **64**, 319–345.